Analytical Study on the Stability of Automobiles under Seismic Motion

Yoshihisa MARUYAMA[1] and Fumio YAMAZAKI[2]

ABSTRACT

The seismometer network of Japanese expressway system has been enhanced since the 1995 Kobe earthquake for more detailed seismic safety monitoring. Using earthquake information from these instruments, the expressways are closed if the peak ground acceleration larger than or equal to 80 cm/s^2 is recorded. However, recent studies on earthquake damage have revealed that expressway structures are not seriously damaged under such level of seismic motion. Hence, we may think of relaxing the regulation of expressway closure. Before doing this, we need to examine the effects of shaking to automobiles on expressways since the drivers may encounter difficulty in controlling their cars and trucks, and traffic accidents may occur. In this study, a vehicle model with six degrees-of-freedom was introduced and its responses were obtained under several seismic motions and the effects of seismic excitation to the dynamic response of the vehicle model were analyzed.

Keywords: vehicle model, seismic response analysis, expressways, driving simulator, yaw angle.

INTRODUCTION

After the 1995 Kobe earthquake, higher priority has been given for the countermeasures against earthquakes than before in Japan. With good financing, thousands of strong motion seismometers were installed. A number of damage assessment systems were also developed by different organizations (Yamazaki et al., 1998). Under this situation, Japan Highway Public Corporation (JH) has developed the new seismometer network along the expressways. Using earthquake information from these instruments, JH closes the expressways if the peak ground acceleration (PGA) larger than or equal to 80 cm/s^2 is recorded (Maruyama et al., 2000). However recent studies on earthquake damage have revealed that expressway structures are not seriously damaged under such level of seismic ground motion (Yamazaki et al., 2000). Though JH closes the expressways under this ground motion level, the serious damages that affect safety driving on expressways are seldom found in the recent years. Hence, we may think of relaxing the regulation of expressway closure.

In this objective, we need to examine the effects of seismic motion to the automobile drivers on expressways since they may encounter difficulties in keeping safety driving and traffic accident may occur. In general, under a large seismic motion, we feel some difficulties to continue doing something that are easily done in the ordinary time, for instance, operating a control system in nuclear power plants. Shibata et al. (1984) tested the accuracy of typing under the strong motion using a computer set on a two-dimensional shaking table. In nuclear plants, a power generation system is controlled by computers and if a large earthquake occurs, operators have to stop the system immediately. They may feel some difficulties in operating the keyboard and switches of the system under intense shaking.

[1] Graduate student, the Institute of Industrial Science, the University of Tokyo
[2] Associate Professor, the Institute of Industrial Science, the University of Tokyo

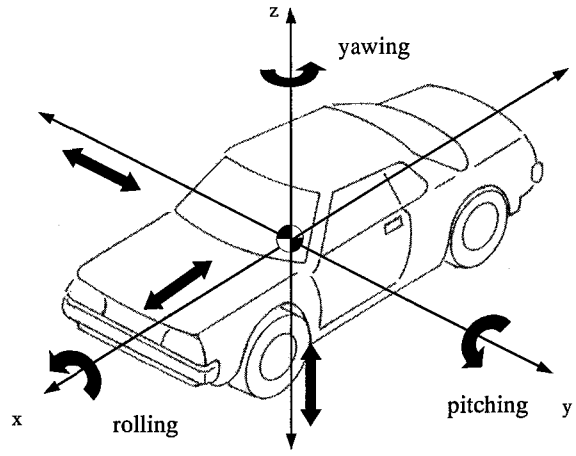

Figure 1. Fundamental motions of a vehicle

Yamanouchi and Yamazaki (1999) investigated drivers' response to strong seismic motion using a driving game machine set on a shaking table. However, the driving game machine used in this experiment has lack of reality as it was made for amusement purpose. Recently, the driving simulators that are concerned with vehicle dynamics are introduced to several organizations (Hiramatsu et al., 1994). In 1999, the driving simulator with six servomotor-powered electric actuators was introduced to the Institute of Industrial Science, the University of Tokyo. Using this driving simulator, we can conduct a series of virtual tests to clarify drivers' responses and their feelings while controlling the simulator under various seismic motions with good reality. Before doing this, we need to investigate the response characteristics of an automobile under various seismic excitations.

In this study, a vehicle model with six degrees-of-freedom, which is used in the driving simulator, was investigated, and its responses under several seismic motions were evaluated. Based on the obtained results, the effects of seismic motion to the dynamic response of a vehicle were investigated.

A VEHICLE MODEL WITH SIX DEGREES-OF-FREEDOM

We define three axes set on the center of gravity of a vehicle. The x-axis is the longitudinal direction, the y-axis is the transverse direction, and the z-axis is the vertical direction of the vehicle. Figure 1 shows the fundamental motions of a vehicle. The model has three translation motions (longitudinal, transverse and vertical) and three rotational motions (rolling, pitching and yawing). Figure 2 shows the two-dimensional coordinate for describing these motions on the *X-Y* plane. In this figure, the *X-Y* coordinate (the absolute coordinate) is independent of the position of a vehicle. The equations of motion of a vehicle to the longitudinal and transverse direction are described as follows:

$$\begin{aligned} m(\dot{u} - vr) &= \sum_j \sum_i \left(F_{xij}\cos\delta_{tij} - F_{yij}\sin\delta_{tij}\right) = \sum_{i,j} F'_{xij} \\ m(\dot{v} + ur) &= \sum_j \sum_i \left(F_{xij}\sin\delta_{tij} + F_{yij}\cos\delta_{tij}\right) = \sum_{i,j} F'_{yij} \end{aligned} \tag{1}$$

where u and v are the velocities in the x and y directions, respectively and r is the angular velocity of yawing. δ is the angle difference between the x-direction and the direction of each tire. F_x and F_y are the longitudinal and transverse forces of each tire, respectively. The index i represents the front or rear wheel and the index j represents the left or right wheel. The yawing motion can be described as

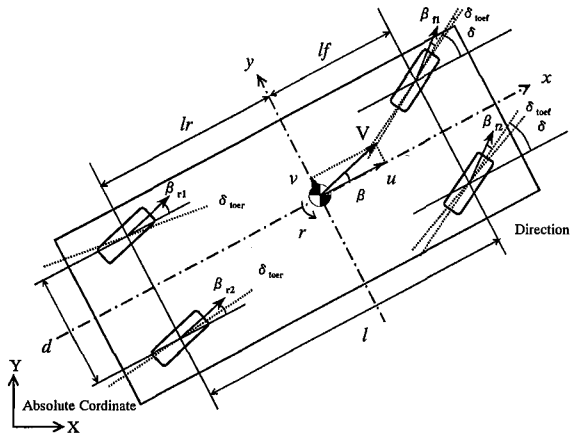

Figure 2. Two-dimensional coordinate on *X-Y* plane

follows:

$$I_z \frac{dr}{dz} = (F'_{y11} + F'_{y12})l_f - (F'_{y21} + F'_{y22})l_r + (-F'_{x11} + F'_{x12})\frac{d}{2} + (-F'_{x21} + F'_{x22})\frac{d}{2} \tag{2}$$

where l_f is the distance between the center of gravity and the front wheel, l_r is the distance to the rear wheel and d is the distance between the right and left wheels. Rolling, yawing and pitching angles are described by Eq. (3), (4) and (5), respectively.

$$\phi = \frac{m(\dot{v} + ur)h}{K_\phi - mgh} \tag{3}$$

$$\psi = \int r dt \tag{4}$$

$$\theta = \frac{m(\dot{u} - vr)h}{2K(l_f{}^2 + l_r{}^2)} \tag{5}$$

where K_ϕ is the rolling stiffness and K is the suspension spring constant.

From Equations (1) to (5), the motions of a vehicle are described in the *x-y* coordinate system set on the center of gravity of a vehicle. The velocities in the absolute coordinate can be defined as

$$\dot{X} = u\cos\psi - v\sin\psi \tag{6a}$$

$$\dot{Y} = u\sin\psi + v\cos\psi \tag{6b}$$

So far, we have described the five kinds of motions out of six. The last one is the vertical motion. In order to describe vertical motion, a quarter vehicle model shown in Fig. 3 is employed (Ellis, 1969). The upper mass represents the body of a vehicle and the lower mass represents a tire. The upper spring is the suspension of a vehicle and the lower spring represents the stiffness of the tire. According to this model, the equation of motion to the vertical direction is described as

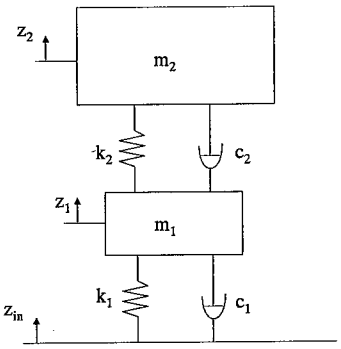

Figure 3. Quarter vehicle model for vertical motion

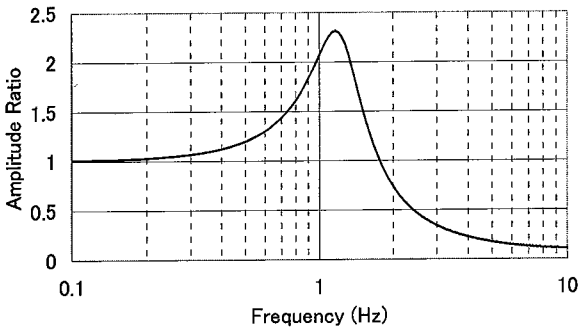

Figure 4. Transfer function of a vehicle to vertical motion

$$m_1(\ddot{\zeta}_1 + \ddot{z}_{in}) + c_1\dot{\zeta}_1 + c_2(\dot{\zeta}_1 - \dot{\zeta}_2) + k_1\zeta_1 + k_2(\zeta_1 - \zeta_2) = 0 \tag{7a}$$

$$m_2(\ddot{\zeta}_2 + \ddot{z}_{in}) + c_2(\dot{\zeta}_2 - \dot{\zeta}_1) + k_2(\zeta_2 - \zeta_1) = 0 \tag{7b}$$

where z_{in} is the vertical displacement of the ground. $\zeta_1 (= z_1 - z_{in})$ and ζ_2 $(= z_2 - z_{in})$ are the relative vertical displacement of m_1 and m_2, respectively.

Substituting proper parameters to Eq. (7), the transfer function between z_{in} and z_2 can be derived. The parameters were set as the same as those used in the driving simulator. The transfer function used in this study is shown in Fig. 4. The predominant frequency is observed at around 1.2 Hz. In order to examine this modeling, the measurements of acceleration were conducted using an actual car (Honda Civic) while it was running. The calculated velocity Fourier spectrum for the vertical component is shown in Fig. 5. In the figure, the predominant frequency is observed at around 1.5 Hz. However these characteristics are, of course, depend on the cars.

SEISMIC RESPONSE ANALYSIS OF THE VEHICLE MODEL

Magic Formula Model

In order to conduct seismic response analysis of a vehicle, we have to calculate the force acting

on each tire. In this study, the Magic Formula Model (Bakker et al., 1989) was employed. Equation (8) shows the fundamental equation used in the Magic Formula Model. All the coefficients used in this equation are determined empirically by some experiments of the manufacturer of the actual driving simulator.

$$y(x) = D\sin\left[C\arctan\left\{Bx - E\left(Bx - \arctan(Bx)\right)\right\}\right]$$

$$Y(x) = y(x) + S_v$$

$$x = X + S_h \qquad \text{(8a, b, c)}$$

where B, C, D and E are the stiffness, shape, peak and curvature factors, respectively. S_h and S_v are the amount of the horizontal and vertical shifts. In the model used in this study, both shifts are set to be zero.

$Y(x)$ in Eq. (8b) is the output force (longitudinal or lateral) of the Magic Formula Model. For calculating the lateral force, F_y, the slip angle is used as the input value X in Eq. (8c). For the longitudinal force, F_x, the slip ratio is used as the input value. The characteristics of the Magic Formula Model used in this study are shown in Fig. 6.

Seismic Response Analysis

In order to conduct the seismic response analysis, Eq. (1) is modified as

$$m_2\left(\dot{u} - vr + \ddot{x}\cos\psi + \ddot{y}\sin\psi\right) = \sum_j\sum_i\left(F_{xij}\cos\delta_{tij} - F_{yij}\sin\delta_{tij}\right) = \sum_{i,j}F'_{xij}$$

$$m_2\left(\dot{v} + ur - \ddot{x}\sin\psi + \ddot{y}\cos\psi\right) = \sum_j\sum_i\left(F_{xij}\sin\delta_{tij} + F_{yij}\cos\delta_{tij}\right) = \sum_{i,j}F'_{yij} \qquad \text{(9a,b)}$$

where $\ddot{x}$ and $\ddot{y}$ are the ground accelerations of longitudinal and transverse directions to the vehicle.

For vertical component, the ground acceleration of the vertical component was substituted as $\ddot{z}_{in}$ in Eq. (7). When pitching and rolling motions occur, the vertical load of the tire will change. The static vertical load of the tire is described as

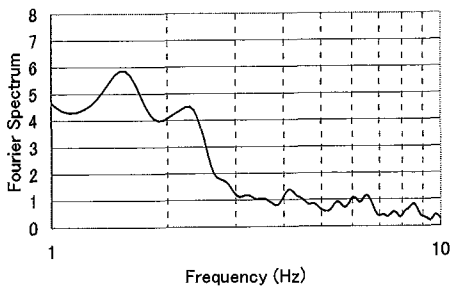

Figure 5. Velocity Fourier spectrum of the vertical component when an actual car was running

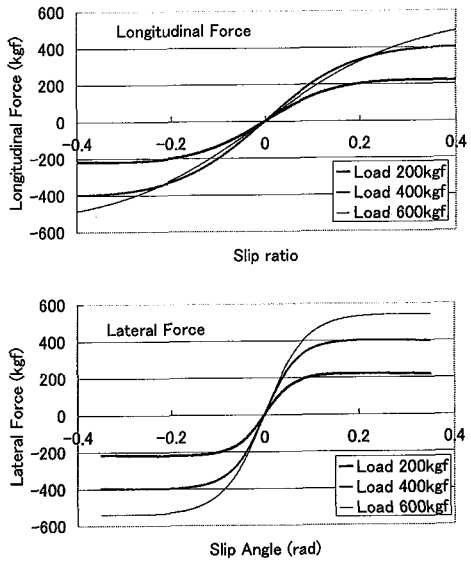

Figure 6. Characteristics of the Magic Formula Model

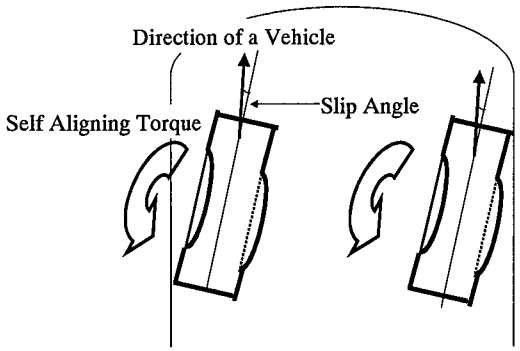

Figure 7. Self aligning torque acting on each tire

$$W_{t0f} = 0.5m_2gl_r/(l_f + l_r) + m_1g/4 \tag{10a}$$

$$W_{t0r} = 0.5m_2gl_f/(l_f + l_r) + m_1g/4 \tag{10b}$$

where f and r represent front and rear respectively. The change of the vertical load due to pitching and rolling motions can be described as

$$W_{tr} = m_2(\dot{v} + ru)h/d \tag{11a}$$

$$W_{tp} = m_2(\dot{u} - rv)h/(l_f + l_r) \tag{11b}$$

where h is the height of the center of gravity. Considering these changes due to pitching and rolling motions, the vertical load of each tire is described as follows:

$$W_{t11} = W_{t0f} - (W_{tp} + W_{tr})/2 \tag{12a}$$

$$W_{t12} = W_{t0f} - (W_{tp} - W_{tr})/2 \tag{12b}$$

$$W_{t21} = W_{t0r} + (W_{tp} - W_{tr})/2 \tag{12c}$$

$$W_{t22} = W_{t0r} + (W_{tp} + W_{tr})/2 \tag{12d}$$

As the vertical motion is considered in this study, the vertical load is also changed due to this motion. Including the change of the load due to the vertical motion, the total vertical load of each tire is described as follows:

$$W_{tij}^{\ total} = W_{tij} - (k_1\zeta_1 + c_1\dot{\zeta}_1) \tag{13}$$

And the height of the center of gravity is changed when the vertical motion occurs. The height of the center of gravity is described as

$$h = h_0 + \zeta_2 \tag{14}$$

where h_0 is the height of the center of gravity under static condition.

The moment called the self aligning torque shown in Fig.7, which reduces the slip angle of each tire, is also considered. This moment reduces the lateral displacement generated by seismic motion.

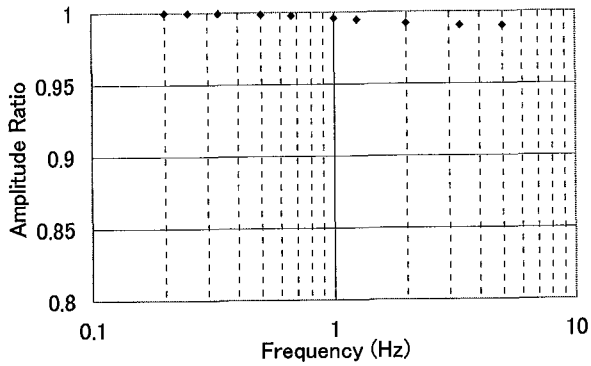

Figure 8. Amplitude ratio and phase delay between input and response accelerations under harmonic excitation

Before conducting the seismic response analysis, the response characteristics of this vehicle model were investigated. The sinusoidal wave with a certain frequency was applied to the transverse direction of the vehicle model and then the absolute response acceleration to the transverse direction was calculated. Figure 8 shows the amplitude ratio between input acceleration and response acceleration. In the figure, when the frequency of the input motion is low, the amplitude ratio between the input and response accelerations is close to 1.0. For higher frequencies, the model shows a little smaller amplitude ratios.

The seismic response analysis was performed using five sets of actual earthquake records. The acceleration records at the Kobe Marine Observatory of Japan Meteorological Agency (JMA) in the 1995 Kobe Earthquake, at the El Centro station in the 1940 Imperial Valley Earthquake (NOAA, 1996), at the K-NET Kofu station in the 2000 Tottori-ken Seibu Earthquake, at SCT station in the 1985 Mexico Earthquake (NOAA, 1996) and at Chiba Experiment Station of Institute of Industrial Science, the University of Tokyo in the 1987 Chiba-ken Toho-Oki Earthquake (Katayama et al., 1990) were selected as typical examples of strong motion records.

Figure 9 shows the acceleration time histories used in this study. Considering the sensitivity of the model (Fig. 8), the filtered motions with the range of 0.2-10 Hz were employed as input motions. Figure 10 shows the acceleration response spectra with 5 % damping for the records (transverse component to the vehicle) scaled to PGA equal to 300 cm/s^2. The acceleration response spectrum of the SCT, Mexico record has much larger value in the frequency range smaller than 1Hz compared with those of the other records. It is also observed that the acceleration spectrum of the El Centro record is larger than those of the JMA Kobe, Tottori and Chiba records in the frequency range smaller than 2Hz.

In order to apply the seismic motion to the vehicle model, the recorded seismic motions were scaled with respect to the peak ground acceleration (PGA). The three-component record was applied to the vehicle model in each case by scaling the records with respect to the PGA of the transverse component. The running speed of a vehicle was set to be 100 km/h.

Figure 11 shows the response of a vehicle due to the seismic motion scaled to 800 cm/s^2 (only for Mexico record, scaled to 300 cm/s^2). As the indices representing the vehicle responses to seismic excitation, the lateral velocity, yaw angular velocity, and lateral displacement were selected. In the figure, it is observed that the response of the vehicle to the El Centro record is larger than those due to the Kobe, Tottori and Chiba records even though all the records were scaled to have the same PGA value. Though the Mexico record was scaled to have the smallest PGA value, the response of the vehicle to the Mexico record is rather large. This is mainly because of the characteristics of the vehicle responses shown in Fig. 8 and the acceleration response spectrum shown in Fig. 10. The vehicle model

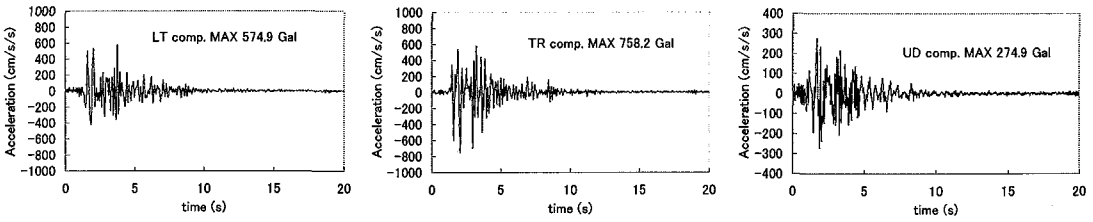

(a) JMA Kobe record

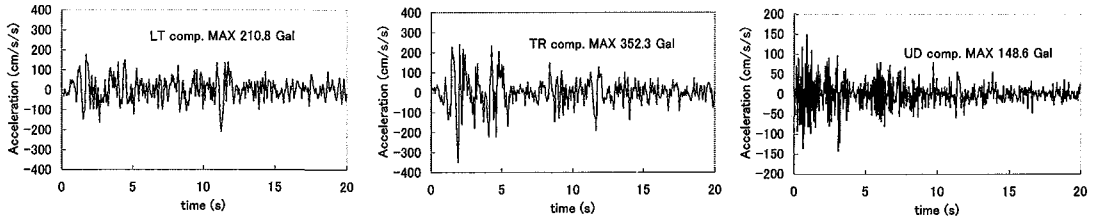

(b) El Centro record

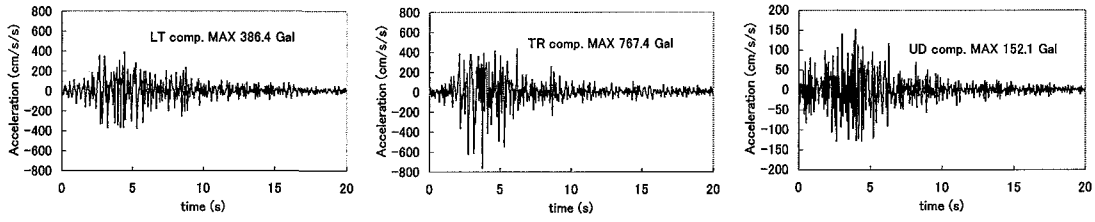

(c) K-NET Kofu, Tottori record

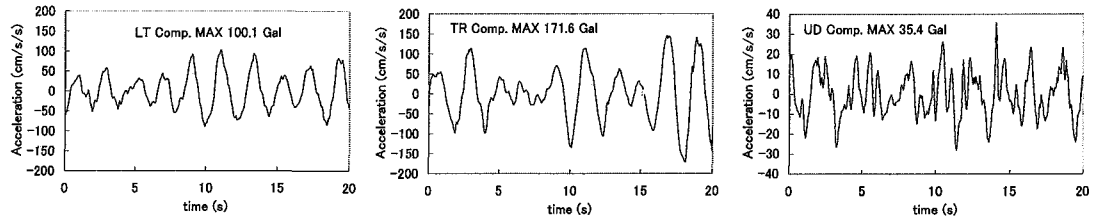

(d) SCT, Mexico record

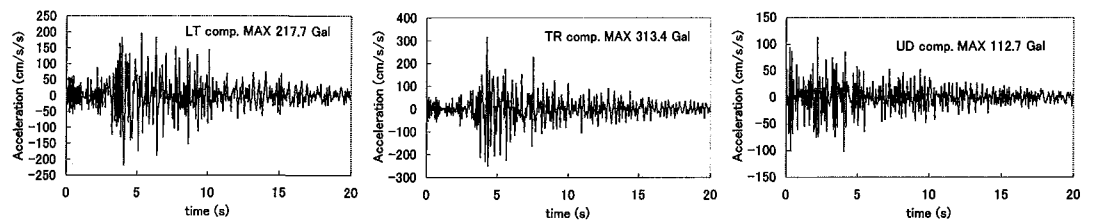

(e) Chiba Experiment Station record

Figure 9. Acceleration time histories used in this study

has high amplitude ratios in the smaller frequency range and the Mexico record has large spectral acceleration in this range. For the lateral displacement of a vehicle, it doesn't become zero but shows

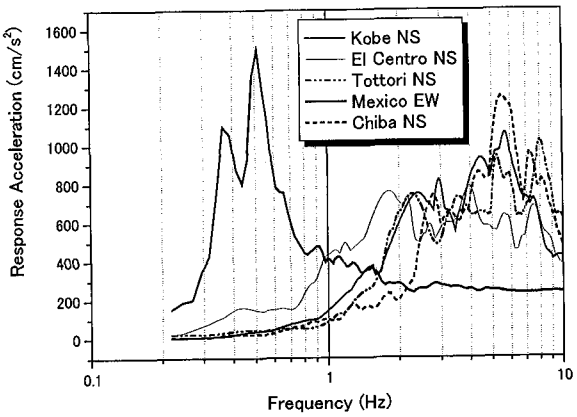

Figure 10. Acceleration response spectra (5 % damping) of five records scaled to PGA=300cm/s^2 applied to the transverse direction to the vehicle

almost straight line. This means that the vehicle has a non-zero yaw angle after the main part of the earthquake.

Figures 12 and 13 show the relationship between the PGA and the maximum lateral velocity and yaw angular velocity for the five sets of acceleration time histories. The running speed of a vehicle was set to be 100 km/h and 120 km/h. These relationships are almost linear and the variation is observed from event to event even the same PGA value was applied. The Mexico and El Centro records were associated by larger lateral velocity responses compared with those by the other three records, and the Mexico record showed much larger yaw angular velocity response than the other records did. It is also observed that, as the running speed of the vehicle becomes large, the vehicle response becomes also large accordingly.

Figure 14 shows the relationship between the peak ground velocity (PGV) and the maximum yaw angular velocity and lateral displacement for the five sets of acceleration time histories. According to the figure, the variations of the maximum values of lateral velocity and yaw angular velocity are not so large from event to event except for the response under the Mexico record. As shown in Fig. 9, the acceleration time history of Mexico record is completely different from the other acceleration time histories. When plotting the vehicle responses as a function of input PGV, the input acceleration of the Mexico record is much smaller than those of the other records. Hence, it is difficult to express various characteristics of seismic motion using only one strong motion index. Except for the Mexico record, which contains long period contents, however, the PGV still seems to be a good index to express ground motion severity from the viewpoint of vehicle response.

Figure 15 shows the relationship between the JMA instrumental seismic intensity (Shabestari and Yamazaki, 1998; Karim and Yamazaki, 2001) and the maximum response of the vehicle. The variations of the responses are very small including the response to the Mexico record. The JMA seismic intensity is calculated through a frequency filtering of a three-component record. This process may have some similarity with the vehicle response model used in this study.

Based on all these results, the JMA intensity may be the most suitable index to express the severity of seismic motion from the viewpoint of vehicle response. However, a further study that considers wider variations in input motion and vehicle parameters may be necessary before the conclusion is made.

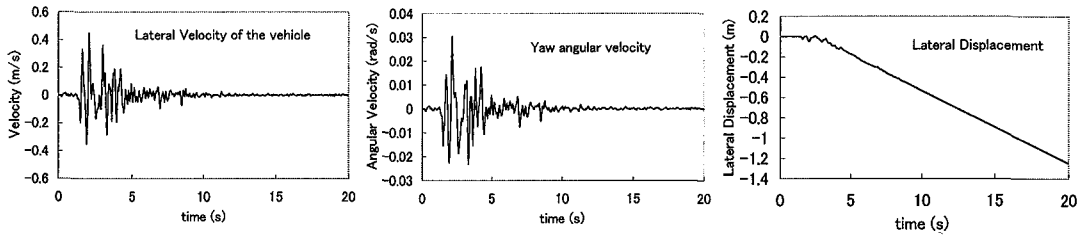

(a) JMA Kobe

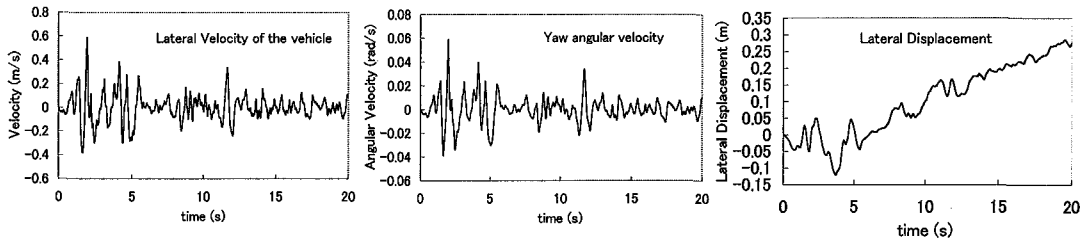

(b) El Centro

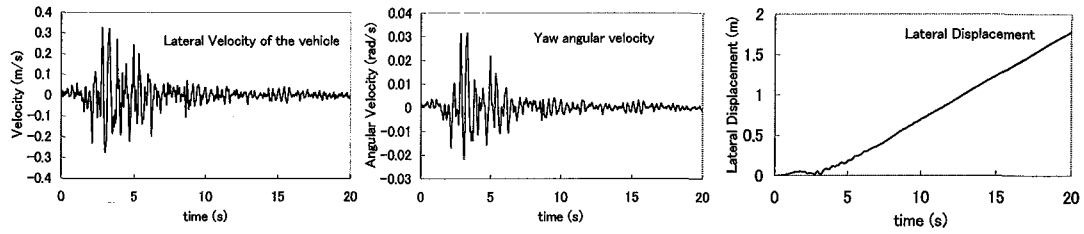

(c) K-NET Kofu, Tottori

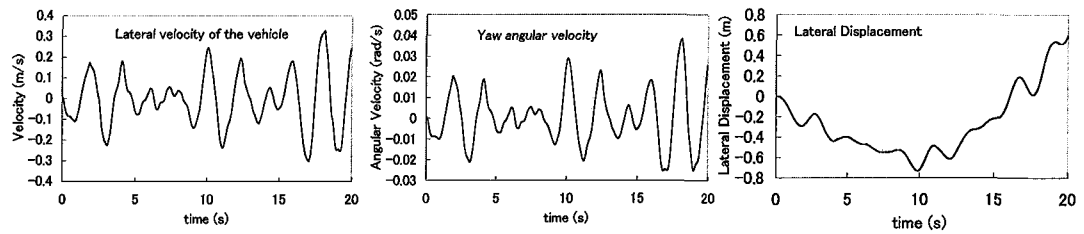

(d) SCT, Mexico

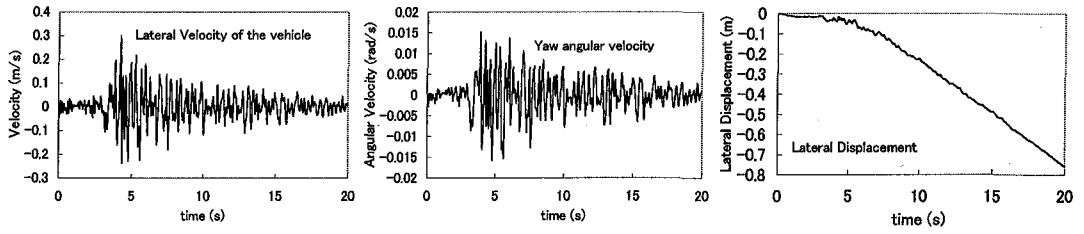

(e) Chiba Experiment Station

Figure 11. Response of a vehicle due to the seismic motions scaled to PGA=800 cm/s^2 (only for Mexico record, scaled to 300 cm/s^2). The initial running speed of the vehicle was set to be 100 km/h.

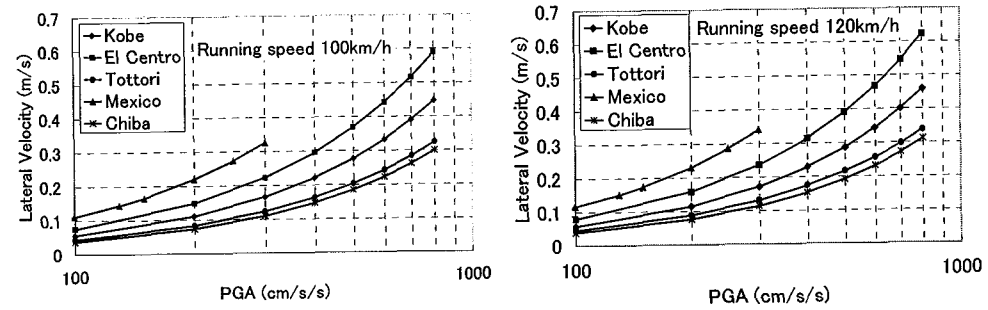

Figure 12. Relationship between the maximum lateral velocity and the peak ground acceleration applied to the transverse direction to the vehicle. The initial running speed of the vehicle is set to be 100 km/h (left) and 120 km/h (right).

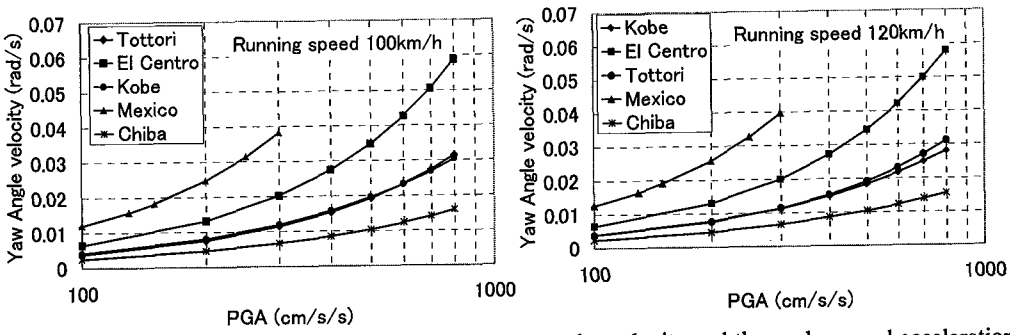

Figure 13. Relationship between the maximum yaw angular velocity and the peak ground acceleration applied to the transverse direction to the vehicle. The initial running speed of the vehicle is set to be 100 km/h (left) and 120 km/h (right).

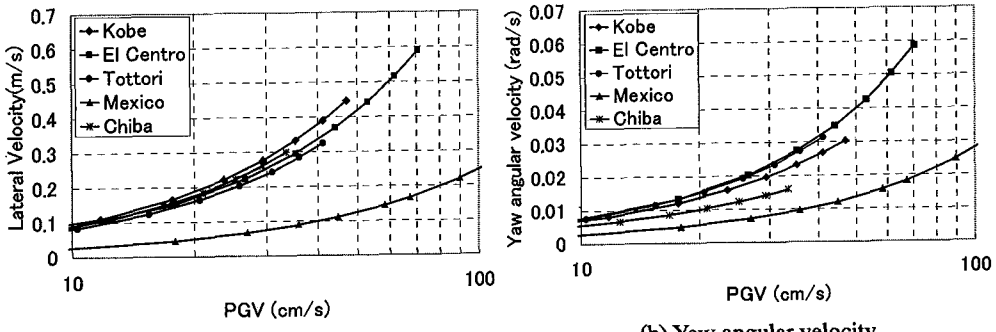

(a) Lateral velocity (b) Yaw angular velocity

Figure 14. Relationship between the maximum response of the vehicle and the peak ground velocity applied to the transverse direction to the vehicle for the initial running 100 km/h

FURTHER STUDY USING DRIVING SIMULATOR

Using the driving simulator shown in Fig. 16, we are planning to conduct a series of virtual tests on highway driving under seismic motion. A scenario highway course is equipped on the simulator for virtual driving. The front view from the driver's seat is realized by three large screens with LCD projectors. The sound system and mirrors give good reality to the simulator. This simulator has six servomotor-powered electric actuators to simulate the motion of a vehicle. Originally, this simulator

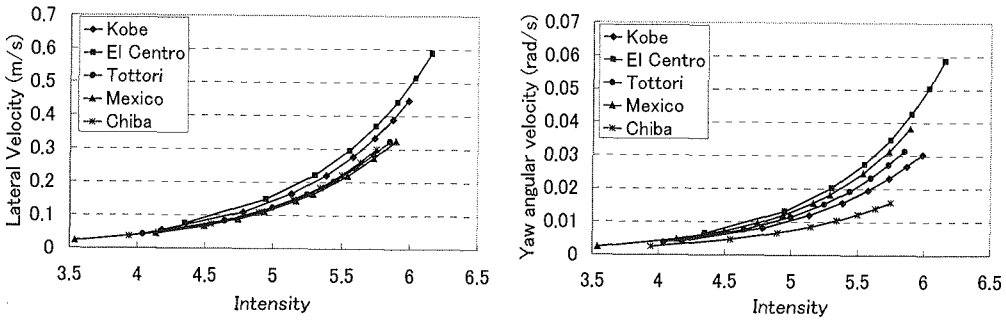

(a) Lateral velocity

(b) Yaw angular velocity

Figure 15. Relationship between the maximum response of the vehicle and JMA intensity applied to the vehicle for the initial running speed 100 km/h

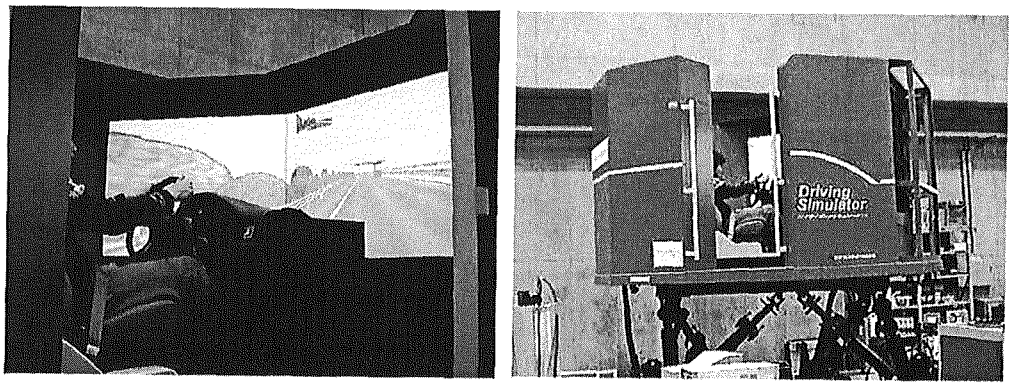

Figure 16. Driving simulator introduced to the Institute of Industrial Science, the University of Tokyo

was designed to simulate the acceleration due to driving a vehicle. We recently modified the control system of the driving simulator such that the seismic motion can be applied to the center of gravity of the vehicle model.

Experiments using this driving simulator can evaluate human reaction to seismic motion properly as well as vehicle dynamics studied in this paper. The virtual driving experiment is expected to give us useful information on the effects of shaking while driving automobiles in high speed, and then it contributes to the promotion of highway safety in natural disasters.

CONCLUSION

In order to investigate the response of an automobile under seismic motion, a vehicle model with six degrees-of-freedom was developed and the seismic response analysis of a running vehicle was carried out. Before conducting the seismic response analysis, the response characteristics of the vehicle were investigated using Magic Formula Model under harmonic excitation having several frequencies. The results of the analysis showed that low frequency motions give larger vehicle response than high frequency motions.

The seismic response analyses were further conducted using five sets of actual earthquake records. The earthquake motions selected in this study were recorded at JMA Kobe Marine

Observatory in the 1995 Kobe Earthquake, at El Centro station in the 1940 Imperial Valley Earthquake, at K-NET Kofu station in the 2000 Tottori-ken Seibu Earthquake, at SCT station in the 1985 Mexico Earthquake, and at Chiba Experiment Station in the 1987 Chiba-ken Toho-Oki Earthquake. The results of the analysis show that as the input seismic motion becomes large, the lateral drift of a vehicle increases. If we set the initial speed of a vehicle larger, the lateral drift becomes also larger accordingly.

The vehicle responses for the different input motions were plotted as a function of peak ground acceleration (PGA). The lateral velocity and yaw angular velocity of the vehicle model were selected as the indices presenting the vehicle response to the seismic excitation. The Mexico and El Centro records were associated by larger lateral velocity responses compared with those by the other three records, and the Mexico record showed much larger yaw angular velocity response than the other records did. Since the Mexico and El Centro records have larger response spectrum amplitudes in the long period range compared with the other records though all records were scaled to have the same PGA value, the response of a vehicle model became larger.

When the relationships between the peak ground velocity (PGV) and the maximum lateral velocity or yaw angular velocity were considered, the relationships were distributed in narrow ranges except for that of the Mexico record. Similar relationships of the vehicle responses were also plotted for the JMA seismic intensity, and the results for the different input motions were very close including that for the Mexico record. According to these results, the JMA intensity may be the most suitable index to express the severity of seismic motion from the viewpoint of vehicle response. However, a further study that considers wider variations in input motion and vehicle parameters may be necessary before the conclusive observation is obtained.

In order to investigate the drivers' responses and their feelings while driving automobiles in high speed under seismic motion, we will conduct series of virtual tests using a driving simulator in the near future. These experiments will contribute to the promotion of expressway safety in natural disasters.

ACKNOWLEDGEMENT

Seismic records used in this study were obtained from the Earthquake Strong Motion CD-ROM by National Geographic Data Center (1989) for the El Centro and the SCT, Mexico records. The JMA Kobe record was provided by Japan Meteorological Agency (JMA) and the K-NET Kofu record from National Research Institute of Earth Science and Disaster Prevention.

REFERENCES

Bakker, E., Pacejka, H. B. & Linder, L. 1989. A new tire model with an application in vehicle dynamics studies. *Society of Automotive Engineering*: No. 890087.

Ellis, J.R. 1969. Vehicle dynamics. *Business Books Ltd.*

Hiramatsu, K., Satoh, K., Uno, H. & Soma, H. 1994. The first step of motion systems realization in the JARI driving simulator. *The International Symposium on Advanced Vehicle Control*: 99-104.

Karim, R.K., Yamazaki F. & Shabestari K.T. 2001. Correlation between the JMA instrumental seismic intensity and strong motions parameters, *Bulletin of Earthquake Resistant Structure Research Center*: No. 34, Institute of Industrial Science, University of Tokyo, 2001.

Katayama, T., Yamazaki, F., Nagata, S., Lu, L. & Turker, T. 1990. A strong motion database for the Chiba seismometer array and its engineering analysis, *Earthquake Engineering and Structural Dynamics*: 19, 8, 1089-1106, 1990.

Maruyama, Y., Yamazaki, F. & Hamada, T. 2000. Microtremor measurements for the estimation of seismic motion along the expressways. *Sixth International Conference on Seismic Zonation*: CD-ROM.

National Oceanic and Atmospheric Administration. 1989. Earthquake Strong Motion CD-ROM, National Geophysical Data Center, Boulder, CO.

Shabestari, K. T. & Yamazaki, F. 1998. Attenuation relationship of JMA seismic intensity using JMA records, *Proc. of the 10th Japan Earthquake Engineering Symposium*, 1, 529-534.

Shibata, H., Ishibatake, H., Fukuda, T. & Komine, H. 1984. Human operability under strong earthquake condition. *Proceedings of the 8th World Conference on Earthquake Engineering*: Vol. V. 1109-1116.

Yamanouchi, H. & Yamazaki, F. 1999. Experiments on the behavior of automobile drivers under seismic motion using driving simulator. *Proceedings of 5th U.S. Conference on Lifeline Earthquake Engineering*: 8-16.

Yamazaki, F., Meguro, K. & Noda, S. 1998. Developments of early earthquake damage assessment systems in Japan. *Structural Safety and Reliability*: 1573-1580.

Yamazaki, F., Motomura, H. & Hamada, T. 2000. Damage assessment of expressway networks in Japan based on seismic monitoring, *12th World Conference on Earthquake Engineering,* CD-ROM, 8p, 2000.